PREPARATION AND CHARACTERIZATION OF HYDROXYAPATITE-MGO NANOCOMPOSITES AND THEIR ANTIMICROBIAL ACTIVITY AND ACUTE TOXICITY

Cho Lwin Lwin Khine[1], San Nwe Zin[2], Ni Ni Sein[3]

Abstract

The application of pure hydroxyapatite (HAp) are restricted to non load-bearing implants due to the poor mechanical properties of hydroxyapatite. To improve the mechanical properties of hydroxyapatite derived from cow bone, incorporation of magnesium oxide was conducted in this research. Hydroxyapatite was prepared by calcination of deproteinised cow bone waste using HCl and NaOH solutions. Magnesium oxide was prepared by wet chemical method treating magnesium nitrate solution with sodium hydroxide solution followed by thermal decomposition of magnesium hydroxide at 600 °C. After addition of magnesium oxide to HAp, the XRD pattern showed the two new peaks corresponding to magnesium oxide peaks at (200) and (220). Crystallite sizes of hydroxyapatite - MgO nanocomposites were 32.17 nm and 37.87 nm for HAp-5 % MgO nanocomposites calcined at 1000 °C and 1100 °C respectively. For HAp-10 % MgO nanocomposites the crystallite sizes were 31.46 nm and 36.70 nm, respectively for calcination temperature of 1000 °C and 1100 °C. Crystal structures of all HAp-MgO nanocomposites and HAp were indexed as hexagonal. FT IR spectral data revealed the characteristics peaks of both hydroxyapatite and MgO in the prepared nanocomposites. HAp-MgO nanocomposites showed mild antimicrobial activities on all tested organisms such as *Bacillus subtilis, Pseudomonas aeruginosa, Candida albicans, Escherichia coli, Staphylococcus aureus and Bacillus pumilus. In vivo* acute toxicity test on albino mice showed no mortality and no toxicity throughout the dosing schedule of 14 days at all dose levels in all groups.

Keywords: hydroxyapatite, magnesium oxide, wet chemical method, hydroxyapatite-MgO nanocomposites, antimicrobial activity, acute toxicity

[1]. 4 PhD, Candidate, Department of Chemistry, University of Yangon
[2]. Dr, Associate Professor, Department of Chemistry, Bago University
[3]. Dr, Professor (Retired), Department of Chemistry, University of Yangon

Introduction

Hydroxyapatite (HAp) is the main biomineral component found in human hard tissues, *i.e*., tooth and bone. Its stoichiometry is represented by the formula ($Ca_{10}(PO_4)_6(OH)_2$). It is comprised of calcium and phosphorus present in the ratio (Ca/P) of 1.67 (Oliveira and Mansur, 2007). It is the main mineral component of the enamel, comprising of more than 60 % of tooth dentin by weight (Goenka *et al*., 2012).

Hydroxyapatite has attracted much interest as a biomaterial for use in prosthetic applications due to its similarity in crystallography and chemical composition to that of human hard tissue. It has outstanding properties like biocompatibility, bioactivity, osteoconductivity, non-toxicity and non-inflammatory nature (Liu *et al*., 1997).

Hydroxyapatite is manufactured in many forms and can be prepared as a dense ceramic, powder, granules, ceramic coating or porous ceramic and various composites as required for the particular applications. However, in recent years, nano-sized hydroxyapatite with appropriate stoichiometry, morphology and purity have a high surface activity and ultrafine structure similar to the mineral found in hard tissues (Sadat-Shojai *et al*., 2013). Hydroxyapatite has got the ability to form a direct chemical bond with living tissues (Sobczak *et al*., 2009).

Synthetic hydroxyapatite can be prepared from an aqueous solution by solid state reaction or by hydrothermal methods (Damien and Revell, 2004). To prepare HAp from those sources needs analytical pure grade chemicals. HAp from natural origins differs from synthetic HAp in composition, crystal morphology, size, shape and physicochemical properties depending on the technology used to obtain the synthetic HAp. Calcination is one of the most used method. Nowadays, natural HAp is prepared (calcination method) from bovine, sheep, pig and goat bones (Sudipo *et al.,* 2012). It is already known that the mechanical properties of HAp are poor, especially in wet environment. For this reason, ceramics of pure HAp cannot be suggested for use in heavy-loaded implants, such as artificial bone or teeth. For improving the mechanical reliability of HAp ceramics, *i.e*., to increase their fracture toughness, incorporation of metallic material, ceramic oxide, whiskers or fibers have been suggested (Demirkol *et al*., 2012).

Magnesium oxide is one of the most successful candidates of reinforcement oxide. Magnesium is also a very important element in human body related to mineralization of calcined tissues, apatite crystallization, destabilization of HAp and thermal conversion of HAp to β-tricalcium phosphate (β-TCP, $Ca_3(PO_4)_2$). Magnesium seemingly reduces risks of cardiovascular diseases, promotes catalytic reactions and controls biological functions of human body (Oktar *et al*., 2007).

Many investigations on the preparation and characterization of hydroxyapatite (HAp) from various aspects have been reported by Myanmar researchers (Thin Thin Nwe, 2005; Than Than Khaing, 2006; Khin Thu Thu Min, 2006; Min Min Than, 2013; Aung Win Thant, 2014 and Zaw Moe Oo, 2014). The present paper is concerned with the preparation and characterization of cow bone HAp-MgO nanocomposites, and investigation of its antimicrobial activity and acute toxicity.

Materials and Methods

The experimental works were conducted at the Department of Chemistry, University of Yangon (UY). Hydroxyapatite (HAp) was prepared from readily affordable biowaste cow bone employing simple unit operations and acid-alkali processes.

Sample Collection

Cow bone samples were collected from Mingalar Taung Nyunt retail market in Yangon Region.

Sample Preparation

Raw cow bone sample worked with distilled water (1 kg) was crushed into splintered bone pieces. It was boiled in a steel pot immersed in 2 L of hot distilled water contained in a steel pot for 4-5 h. Boiling was repeated 3 more times. The boiled sample (800 g) was then pressure cooked in 2 L of distilled water, under pressure of 5-7.5 psi. Pressure cooking was repeated 3 more times with fresh distilled water. Washing, boiling and pressure cooking removed any adhering oil, fat, meaty things plus some contaminated dirt and

microorganisms. Dried bone pieces were then treated with 1M HCl (2 L) in a glass tank for about 24 h accompanied by occasional stirring. After the acidification, bone pieces were washed with distilled water to a nearly neutral state (pH 6.5-7.3) the bone pieces were then immersed in 2 L of 1 M NaOH for about 24 h. The alkali treated bone pieces were repeatedly washed with distilled water to a neutral state. It was air dried and pulverized to a powder form (44 μm). The acid-alkali treatment removed any remaining tissue, fatty matter and making the splintered bones more porous and brittle. It aided the splintered bones to be ground to the powder form. The hydroxyapatite powder was calcined at 900 °C in a muffle furnace.

Synthesis of Magnesium Oxide Nanoparticles

Magnesium oxide nanoparticles were prepared by wet chemical method using magnesium nitrate hexahydrate and sodium hydroxide as precursors and soluble starch as stabilizing agent. Starch act as a stabilizing agent and also prevents the agglomeration of nanoparticles (Agrawal *et al*., 2015). Starch (0.1 % concentration) solution was prepared in 100 mL of distilled water and magnesium nitrate 0.4 mol was added to the above solution. Then the solution was kept under constant stirring using magnetic stirrer for complete dissolution of contents. After complete dissolution, 0.8 mol of sodium hydroxide solution was added in drops along the sides of the container under constant stirring for 2 h and allowed to settle for 24 h. The supernatant liquid was then discarded carefully and the remaining solution was centrifuged (3000 rpm at 25 °C) for 30 min. Centrifugate was washed three times using distilled water and ethanol to remove the by-products and the excessive starch that bound with the nanoparticles. The nanoparticles of magnesium hydroxide were dried in an oven at 100 °C for 4 h and annealed in a muffle furnace at 600 °C for 4 h to obtain magnesium oxide. During this process, conversion of magnesium hydroxide into magnesium oxide took place.

Synthesis of Hydroxyapatite-MgO Nanocomposites

MgO (5 g) was dispersed in 20 mL of distilled water with the help of a magnetic stirrer for 1 h. The hydroxyapatite suspension was also prepared using the ratio of 1:1 for powder (100 g) and water (100 mL) by means of magnetic stirring for 1 h to get homogeneity of the dispersion. In order to prepare HAp-MgO nanocomposites, the weight percentages (wt %) of 5 and 10 were chosen. The prepared MgO suspension was poured into the HAp solution and then was thoroughly mixed using stirrer at 80-90 °C for 1 h. The obtained suspension was cooled to room temperature for 12 h. In addition, it was filtered using a funnel through filter paper. The residues were washed 2 to 3 times with distilled water. Then, it was transferred into porcelain basin and placed in an oven at 120 °C for 4 h to obtain dried sample. Moreover, the resulting products were annealed at 1000 °C and 1100 °C for 4 h.

Characterization Techniques

TG-DTA (DTG-60 H) Thermal Analyzer, Shimadzu, Japan was employed for investigation of the thermal property of prepared magnesium oxide and cow bone hydroxyapatite. The sample was scanned from 40 °C to 600 °C under nitrogen atmosphere with a flow rate of 50 mL min^{-1}. The techniques employed were in accordance with the company's catalogue.

Phase analysis and purity of prepared magnesium oxide, hydroxyapatite and hydroxyapatite-MgO nanocomposites obtained were investigated by X-ray analysis. X-ray diffraction patterns of the samples were recorded on X-ray diffractometer (Rigaku, Tokyo, Japan), using CuK_α radiation (λ= 1.54 Å) at 40 kV and 40 mA. The diffraction angle ranged from 10^o to 70^o of 2θ. The crystallite size was calculated by Scherrer method. The crystallinity percent was obtained by dividing total area of crystalline peaks by total area of all peaks.

Fourier transform infrared (FT IR) spectra of the samples was recorded on a FT IR spectrometer (FT IR-8400 SHIMADZU, Japan). FT IR analysis was in a range of wavenumber from 4000 to 440 cm^{-1}.

The morphology of the samples were observed by scanning electron microscopy (JEOL-JSM 5610 LV, Japan).

In vitro Investigation of Antimicrobial Activity of HAp-MgO Nanocomposites

Antimicrobial activities of HAp-MgO nanocomposites were tested by agar well diffusion method at Pharmaceutical Research Department (PRD), Yangon. The microorganism selected were *B. subtilis*, *S. aureus*, *P. aeruginosa*, *B. pumilus*, *C. albicans* and *E. coli*. Nutrient agar was prepared according to method described by Cruickshank (1975). Briefly, nutrient agar was boiled and 20-25 mL of the medium was poured into a test tube and plugged with cotton wool and autoclaved at 121 °C for 15 min. Then the tubes were cooled down to 60 °C and poured into sterile petri dish and 0.1 mL of spore suspension was also added into the dishes. The agar was allowed to set for 30 min after which 10 mm plate agar well was made with the help of sterilized cork borer. After that, about 0.1 mL of sample was introduced into the agar well and incubated at 37 °C for 24 h. The inhibition zone (clear zone) appeared around the agar well indicated the presence of antimicrobial activity. The extent of antimicrobial activity was measured from the zone of inhibition diameter.

In vivo Acute Toxicity Test of HAp-MgO Nanocomposites

Acute toxicity of HAp-MgO nanocomposites was tested according to the methods of OECD Guidelines for the Testing of Chemicals 423 at Laboratory Animal Services Division, Department of Medical Research (DMR), Yangon.

According to the test description, total number of 54 adult albino mice, weighing (25-30 g) were selected and divided into 9 groups. Each group contained six animals. They were fasted for 18 h before giving the HAp-MgO nanocomposites. Group (A 1 to D 2) mice were orally administered with HAp-MgO nanocomposites 2000 mg/kg dose and 5000 mg/kg dose (Figure 1). Group (E) mice performed as a control group and they were treated with clean water and normal animal food. All groups of mice were kept in the standard aluminium mouse cages and allowed to access food and water in the separate room at the room temperature of 26 ±1ºC. After administration, mortality and behaviour changes were continuously observed. Then the

animals were checked each 24 h for fourteen days. The mortality during this period was noted (Nil or percent death).

(a) Weighing albino mice

(b) Oral administration of HAp-MgO nanocomposite

Figure 1: Acute toxicity test on albino mice

Results and Discussion

TG-DTA Analysis

TG-DTA thermograms of magnesium hydroxide and magnesium oxide are shown in Figures 2 and 3. One decomposition step was observed in TG-DTA thermogram of magnesium hydroxide with a sharp endothermic peak appeared at 335.28 °C because of phase transition from magnesium hydroxide to magnesium oxide. The weight loss is 30.86 % which is in agreement with the theoretical weight loss of water (31.03 %). TG-DTA thermogram of magnesium oxide at 600 °C for 4 h showed a very small endothermic peak around at 280 °C due to loss of water. Furthermore, TG-DTA thermograms of HAp-MgO nanocomposites at 1000 °C and 1100 °C are shown in Figures 4, 5, 6 and 7 and thermal data are presented in Table 1. No inflection of TG curve with small weight loss was observed in each TG curved of HAp-MgO nanocomposites indicating the stability of the sample.

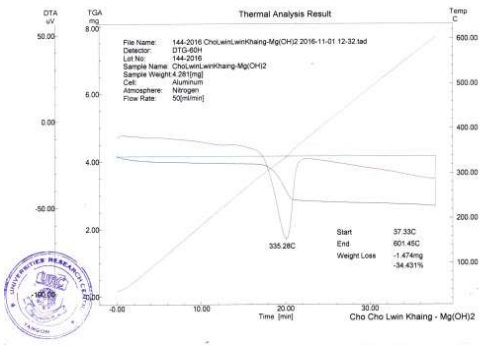

Figure 2: TG-DTA thermogram of magnesium hydroxide

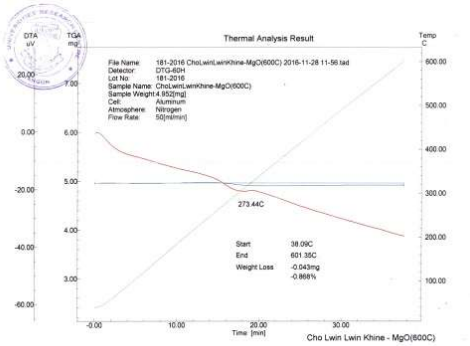

Figure 3: TG-DTA thermogram of magnesium oxide at 600 °C

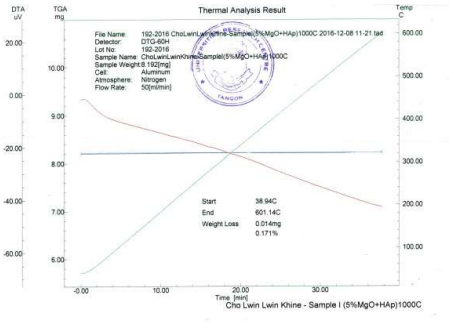

Figure 4:TG-DTA thermogram of HAp-5 % MgO at 1000 °C

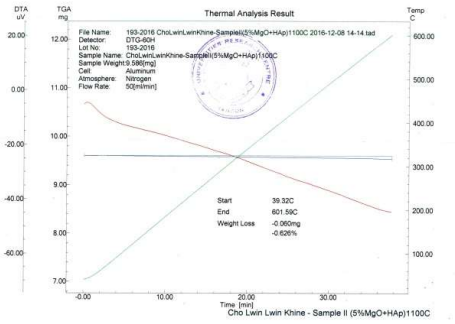

Figure : TG-DTA thermogram of HAp-5 % MgO at 1100 °C

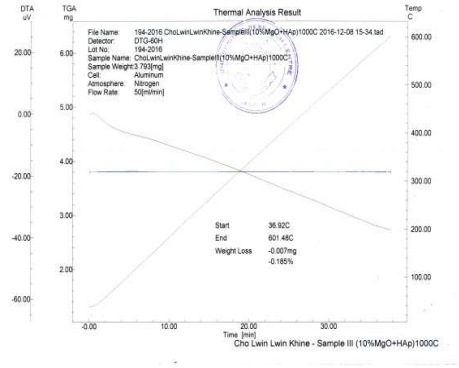

Figure 6: TG-DTA thermogram of HAp-10 % MgO at 1000 °C

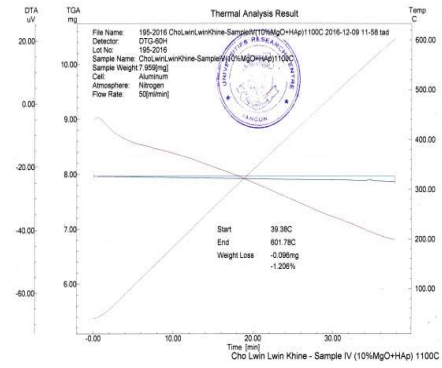

Figure 7: TG-DTA thermogram of HAp-10 % MgO at 1100 °C

Table 1: Thermal Analysis Data of Hydroxyapatite-MgO Nanocomposites

Sample	Temperature range (°C)	Initial weight (mg)	Final weight (mg)	Weight loss (%)	Remark
HAp-5 % MgO 1000 °C	38.94-601.14	8.192	8.178	0.171	Thermally stable
HAp-5 % MgO 1100 °C	39.32-601.59	9.586	9.526	0.626	Thermally stable
HAp-10 % MgO 1000 °C	36.92-601.48	3.793	3.786	0.185	Thermally stable
HAp-10 % MgO 1100 °C	39.38-601.78	7.959	7.863	1.206	Thermally stable

XRD Analysis

The well-resolved XRD pattern of hydroxyapatite (Figure 8) could be easily indexed on the basis of hexagonal crystal system with equal length of a and b axes (a=b= 9.4009 Å) and shorter length of c axis (c= 6.8757Å). The mean crystallite size of hydroxyapatite sample has been estimated from full width at half maximum (FWHM) and Scherrer equation according to the following formula:

$$\tau = \frac{0.9\,\lambda}{\beta \operatorname{Cos} \theta}$$

where τ is the crystallite size (nm), λ is the diffraction wavelength (0.154056 nm for Cu K_α radiation), θ is the diffraction angle (degree) and β is the full width at half maximum (FWHM) for the diffraction peak (radian). The prepared magnesium oxide samples were subjected to XRD analysis and three well-defined diffraction peaks were observed in each diffractogram at Miller indices of (111), (220) and (200) (Figure 9). A single phase of magnesium

oxide with face-centered cubic structure and space group of Fm3m was observed from XRD analysis. After addition of magnesium oxide to hydroxyapatite, the XRD patterns of HAp-MgO nanocomposites showed two new peaks corresponding to magnesium oxide peaks at (200) and (220) (Figure 10). Crystallite sizes of prepared magnesium oxide was found to be 21.71 nm and crystallinity of magnesium oxide is 54.39 % (Table 2). For hydroxyapatite, the crystallite size and crystallinity percent are 78.24 nm and 63.51 %. Crystallite sizes of HAp-MgO nanocomposites were 32.17 nm and 37.87 nm for HAp-5 % MgO nanocomposites calcined at 1000 °C and 1100 °C respectively. For HAp-10 % MgO nanocomposites the crystallite sizes were 31.46 nm and 36.70 nm, respectively, for calcination temperature of 1000 °C and 1100 °C. Crystallinity values of HAp-5 % MgO nanocomposites were 70.65 and 76.49 % and those of HAp-10 % MgO nanocomposites were 68.12 % and 75.39 %, respectively, at 1000 °C and 1100 °C. With increase in temperature the crystallite size and percent crystallinity of HAp-MgO nanocomposites were found to increase. However, the results were reversed as the amount of magnesium oxide was increased. Moreover, peak positions were slightly shifted to lower positions as the temperature increased from 1000°C to 1100°C (Table 3). Crystal structures of all HAp-MgO nanocomposites and HAp were hexagonal and that of MgO was cubic. Comparison of lattice constants of hydroxyapatite, magnesium oxide and HAp-MgO nanocomposites is shown in Table 4. The lattice constants of HAp-MgO nanocomposites noticeably changed from those of HAp and MgO indicating the formation of composite. Among the HAp-MgO nanocomposites, the lattice constants changed slightly with change in temperature and amount of magnesium oxide.

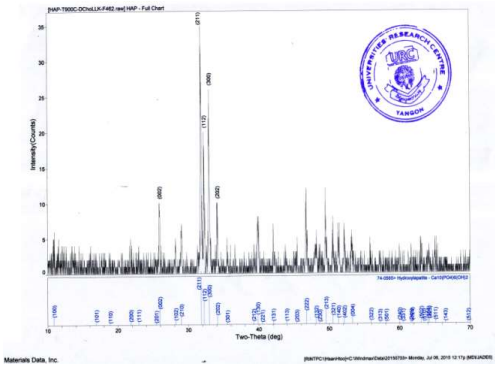

Figure 8: X-ray diffractogram of hydroxyapatite

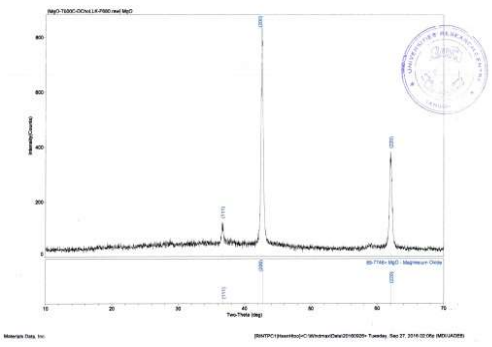

Figure 9: X-ray diffractogram of magnesium oxide at 600 °C

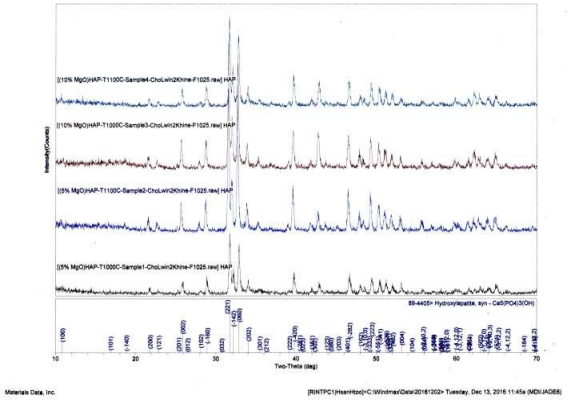

Figure 8: X-ray diffractogram of hydroxyapatite

Table 2: Average Crystallite Sizes and Crystallinity Percents of HAp, MgO and HAp-MgO Nanocomposites

No	Samples	Average crystallite size (nm)	Crystallinity (%)
1	HAp	78.24	63.51
2	MgO	21.71	54.39
3	HAp-5 % MgO Nanocomposite at 1000 °C	32.17	70.65
4	HAp-5 % MgO Nanocomposite at 1100 °C	37.87	76.49
5	HAp-10 % MgO Nanocomposite at 1000 °C	31.46	68.12
6	HAp-10 % MgO Nanocomposite at 1100 °C	36.70	75.39

Table 3: Changes of Peak Positions of HAp-MgO Nancomposites at Different Concentrations of MgO and Different Temperatures

Peak position 2 θ (degree)				Miller Indices hkl	Remark
HAp-5 % MgO 1000 °C	HAp-5 % MgO 1100 °C	HAp-10 % MgO 1000 °C	HAp-10 % MgO 1100 °C		
25.853	25.632	25.772	25.663	002	HAp
31.743	31.548	31.660	31.576	221	HAp
32.169	31.967	32.078	31.987	142	HAp
32.865	32.680	32.788	32.712	060	HAp
39.760	39.588	39.667	39.607	420	HAp
42.852	42.749	42.841	42.745	220	MgO
62.372	62.119	62.165	62.140	200	MgO

Table 4: Comparison of Lattice Costants of HAp, MgO and HAp-MgO Nanocomposites

Sample	Lattice Constants (Å)			Crystal structure
	a	b	c	
HAp	9.4009		6.8757	Hexagonal
HAp-5 % MgO at 1000 °C	9.5469		6.8434	Hexagonal
HAp-5 % MgO at 1100 °C	9.5998		6.9544	Hexagonal
HAp-10 % MgO at 1000 °C	9.5650		6.7985	Hexagonal
HAp- 10 % MgO at 1100 °C	9.5295		6.8878	Hexagonal
MgO	4.2357	4.2357	4.2357	Cubic

FT IR Analysis

FT IR spectra of hydroxyapatite, magnesium oxide and HAp-MgO nanocomposites with different MgO percents at 1000 °C and 1100 °C are shown in Figures 11 to 16. FT IR spectral data revealed the characteristics peaks of both hydroxyapatite and MgO in the prepared nanocomposites (Table 5). The characteristics peaks of hydroxyapatite in nanocomposites were observed between 700-400 cm^{-1} due to P-O bending vibration and between 1200-900 cm^{-1} due to P-O stretching vibration. Similarly, the characteristics peaks of MgO in nanocomposites were observed at 441 cm^{-1} and between 650-440 cm^{-1}due to MgO bending vibration.

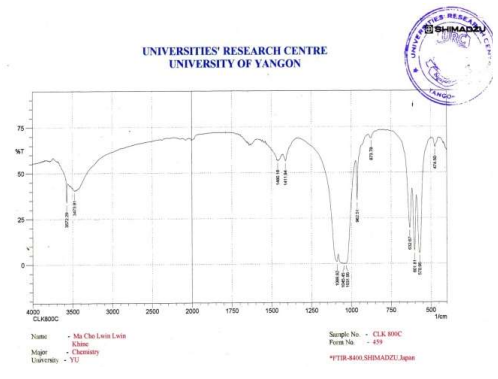

Figure 11: FT IR spectrum of hydroxyapatite

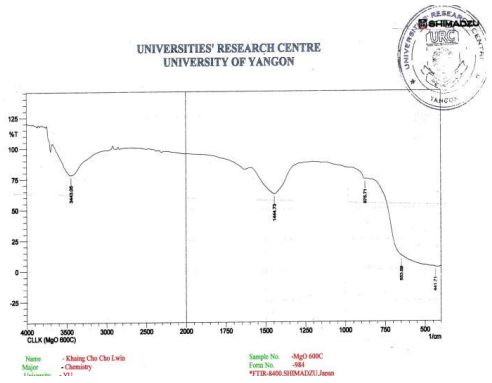

Figure 12: FT IR spectrum of magnesium oxide at 600 °C

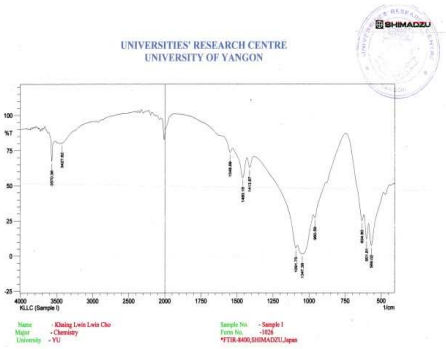

Figure 13: FT IR spectrum of HAp-5 % MgO at 1000 °C

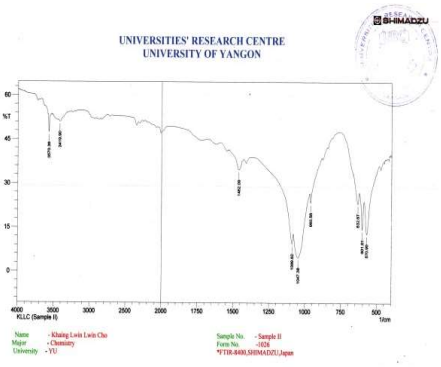

Figure 14: FT IR spectrum of HAp-5 % MgO at 1100 °C

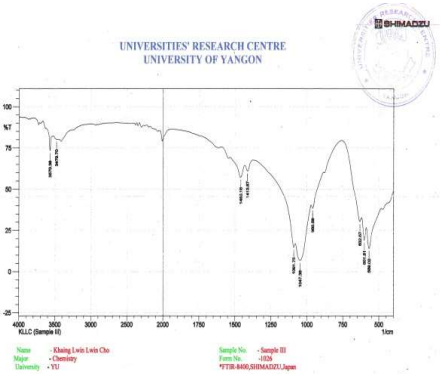

Figure 15: FT IR spectrum of HAp-10 % MgO at 1000 °C

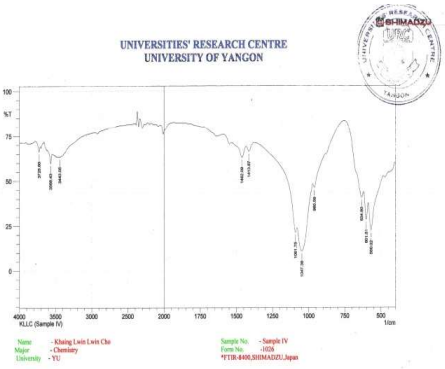

Figure 16: FT IR spectrum of HAp-10 % MgO at 1100 °C

Table 5: FT IR Spectral Data of HAp, MgO and HAp-MgO Nanocomposites

No	HAp	MgO	Wavenumber (cm^{-1})				Reported Values (cm^{-1})	Remark
			5 % MgO at 1000 °C	5 % MgO at 1100 °C	10 % MgO at 1000 °C	10 % MgO at 1100 °C		
1	3697		3570	3570	3510	3568	3500-3100*	Vibration of O-H
2	3443		3427	3419	3479	3443		
3		3440					3444**	O-H stretching vibration of physically adsorbed water molecules
4	1456		1460	1462	1460	1462	1629-1400*	Carbonate group
5	1413		1413		1413	1413		
6		1444					1600-1400**	O-H bending vibration of physically absorbed water molecules
7	1089		1091	1089	1091	1091	1200-900*	P-O stretching of phosphate
8	1047		1047	1047	1047	1047		
9	962		960	960	960	960		
10	877						871*	Carbonate group
11		653					650-450**	Mg-O deformation vibration
12	632		632	632	632	634	700-500*	P-O bending of phosphate
13	601		601	601	601	601		
14	570		569	570	569	569		
15	474	474	472	474	474	474	650-450**	Mg-O deformation vibration

* Nakamoto, 1970 ** Karthikeyan *et al.,* 2016

SEM Analysis

SEM images depict that magnesium oxide nanoparticles are appearing as spherical granule with slight agglomeration (Figure 17). Microscopic observations illustrated that the HAp-5 % MgO nanocomposite calcined at 1000 °C showed elongated shape. As the concentration of MgO increased, irregular shape are observed. Increasing temperature to 1100 °C, the poorly connected particles tend to agglomerate.

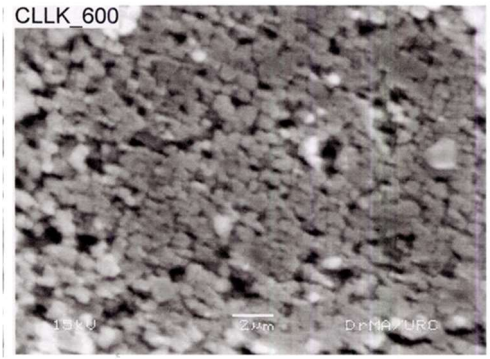

Figure 17: SEM image of magnesium oxide at 600 °C

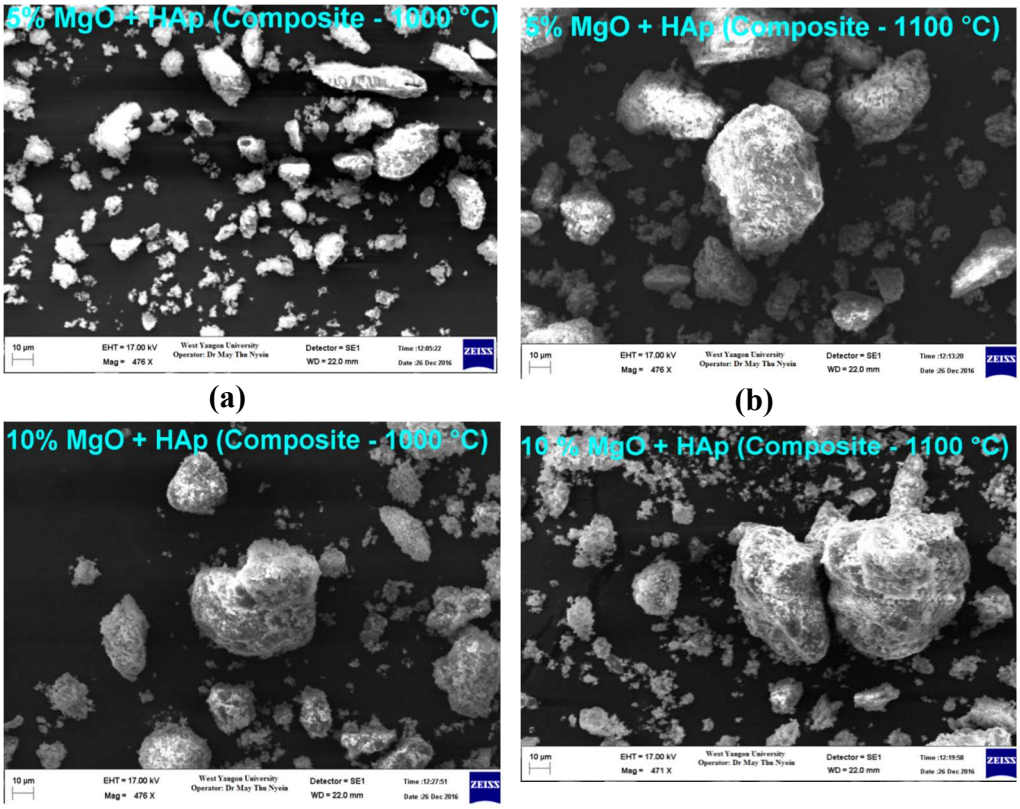

Figure 18: SEM images of HAp-5 % MgO nanocomposite at (a) 1000 °C (b) 1100 °C and HAp-10 % MgO nanocomposite at (c) 1000 °C (d) 1100 °C

Antimicrobial Activity of HAp-MgO Nanocomposites

Antimicrobial activities of HAp-MgO nanocomposites (5 % and 10 %) were investigated against six microorganisms. HAp-MgO nanocomposites (5 % and 10 %) only showed mild antimicrobial activities on all tested organisms such as *Bacillus subtilis, Pseudomonas aeruginosa, Candida albicans, Escherichia coli, Staphylococcus aureus and Bacillus pumilus* (Table 6).

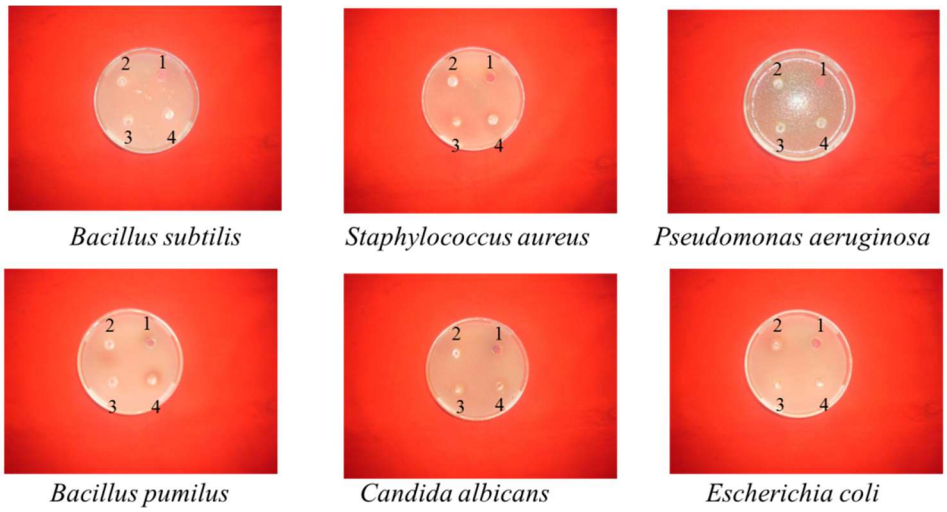

1 = control
2 = HAp
3 = HAp-5 % MgO at 1000 °C
4 = HAp-5 % MgO at 1100 °C

Figure 19: Antimicrobial activity of HAp and HAp-5 % MgO nanocomposites with six tested microorganisms

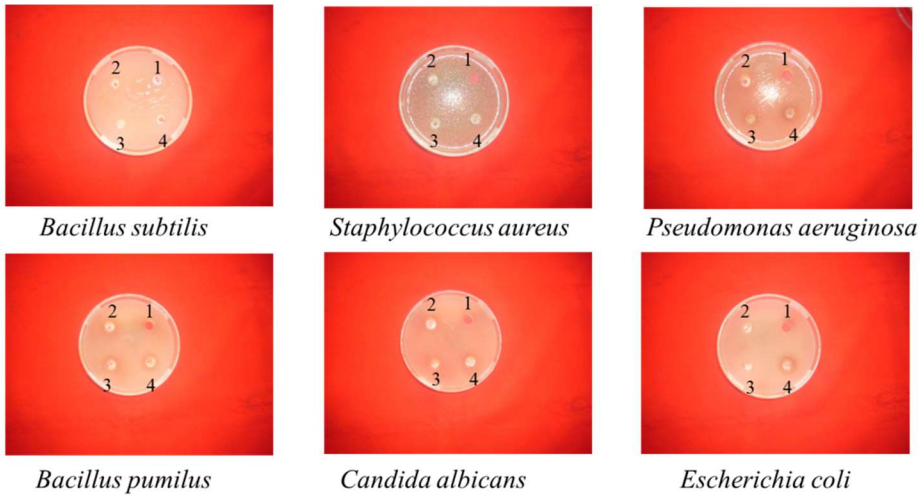

Figure 20: Antimicrobial activity of HAp and HAp-10% MgO nanocomposites with six tested microorganisms

Table 6: Antimicrobial Activities of HAp-MgO Nanocomposites

Samples	Inhibition Zone Diameters (mm)					
	B. subtilis	***S. aureus***	***P. aeruginosa***	***B. pumilus***	***C. albicans***	***E. coli***
Control	DW	DW	DW	DW	DW	DW
HAp	12	12	12	12	12	12
HAp-5 % MgO at 1000 °C	13 mm (+)	13 mm (+)	12 mm (+)	12 mm (+)	13 mm (+)	13 mm (+)
HAp-5 % MgO at 1100 °C	13 mm (+)	13 mm (+)	12 mm (+)	13 mm (+)	13 mm (+)	13 mm (+)
HAp-10 % MgO at 1000°C	13 mm (+)	12 mm (+)	13 mm (+)	12 mm (+)	13 mm (+)	12 mm (+)
HAp-10 % MgO at 1100°C	13 mm (+)	12 mm (+)	13 mm (+)	13 mm (+)	13 mm (+)	13 mm (+)

Agar well – 10 mm
10 mm ~ 14 mm (+)
15 mm ~ 19 mm (++)
20 mm above (+++)

Acute Toxicity Tests of HAp-MgO Nanocomposites on Albino Mice Model

Acute toxicity screening of HAp-MgO nanocomposite was done with the dosage of 2000 mg/kg and 5000 mg/kg body weight in each group of albino mice. The condition of mice groups were recorded after fourteen days administration. No lethality of the mice was observed until 2 weeks with the maximum dose of administration (Table 7). Each group of animals was also observed still alive and did not show any visible symptoms of toxicity like restlessness, respiratory disorders, convulsion, aggressive activities, coma and death. Even with the dose up to 2000 mg/kg and 5000 mg/kg body weight administration, there was no lethality at the day of fourteen.

Table 7: Results of Acute Toxicity Study of HAp-MgO Nanocomposites on Albino Mice Model

Group	Dose (mg/kg)	No. of mice tested	Observed periods (d)	Death per test
A 1	2000	6	14	0/6
A 2	5000	6	14	0/6
B 1	2000	6	14	0/6
B 2	5000	6	14	0/6
C 1	2000	6	14	0/6
C 2	5000	6	14	0/6
D 1	2000	6	14	0/6
D 2	5000	6	14	0/6
E (Control)	-	6	14	0/6

A 1, A 2 = HAp-5 % MgO at 1000 °C C 1, C 2 = HAp-10 % MgO at 1000 °C

B 1, B 2 = HAp-5 % MgO at 1100 °C D 1 D 2 = HAp-10 % MgO at 1100 °C

Conclusion

HAp-MgO nanocomposites were successfully prepared in this research. TG-DTA analysis showed the stability of the HAp-MgO nanocomposites. Higher temperatures lead to higher percent crystallinity resulting in with increasing crystallite sizes. Decrease in MgO content caused the lower percent crystallinity and crystallite size. FT IR spectral data revealed the presence of characteristic peaks of both MgO and HAp in HAp-MgO nanocomposites. On addition of magnesium oxide content and increase in temperature, peak position slightly shifted to lower positions. The shift indicated the change in morphology and crystal orientation. Hydroxyapatite-MgO nanocomposites have mild activity on six tested microorganisms. *In vivo* acute toxicity test revealed that no lethality of the albino mice was observed oven up to fourteen days of administering.

Acknowledgements

The authors would like to express their profound gratitude to the Department of Higher Education (Yangon Office), Ministry of Education, Myanmar for provision of opportunity to do this research.

References

Agrawal, R. M., Charpe, S. D., Raghuwanshi, F. C. and Lamdhade, G. T. (2015). "Synthesis and Characterization of Magnesium Oxide Nanoparticles with 1:1 Molar Ratio via Liquid-Phase Method". *International Journal of Application or Innovation in Engineering and Management,* vol. 4(2), pp.141-144

Aung Win Thant. (2014). *Preparation and Characterization of Hydroxyapatite from Fish Bone*. MSc Thesis, Department of Chemistry, University of Yangon

Cruickshank, R. (1975). *Test for Sensitivity to Antimicrobial Agents in Medical Microbiology*. Edinburgh: 12th Edition, Churchill Livingston Publication, pp.120-122

Damien, E. and Revell, P. A. (2004). "Coralline Hydroxyapatite Bone Graft Substitute; A Review of Experimental Studies and Biomedical Application". *Journal of Applied Biomaterials and Biomechanics*, vol. 2, pp. 65-73

Demirkol, N., Meydanoglu, O., Gokce, H., Oktar, F. N. and Kayali, E. S. (2012). "Comparison of Mechanical Properties of Sheep Hydroxyapataite (SHA) and Commercial Synthetic Hydroxyapatite (CSHA)-MgO Composites". *Key Engineering Material.,* vol. 493-494, pp. 588-593

Goenka, S., Balu, R. and Sampath, K. T. S. (2012). "Effects of Nanocrystalline Calcium Deficient Hydroxyapatite Incorporation in Glass Ionomer Cements". *J Mech Behav Biomed Mater*., vol. 7, pp. 69-76

Karthikeyan, V., Dhanapandian, S. and Manoharan, C. (2016). "Characterization and Antibacterial Behavior of MgO Nanoparticles Synthesized via Co-precipitation Method". *International Journal for Scientific Research and Development,* vol. 10(1), pp. 2321-2323

Khin Thu Thu Min. (2006). *Studies of Bioceramics Iron and Zinc Substituted Hydroxyapatites*. PhD Dissertation, Department of Chemistry, University of Yangon

Liu, C., Wang, W., Shen, W., Chen, T., Hu, L. and Chen, Z. (1997). "Evaluation of the Biocompatibility of A Nonceramic Hydroxyapatite". *J Endod*., vol. 23, pp. 490-493

Min Min Than. (2013). *Removal of Some Heavy Metal Ions by using Synthetic Carbonate Hydroxyapatit*e. PhD Dissertation, Department of Chemistry, University of Yangon

Nakamoto, K. (1970). *Infrared Spectra of Inorganic and Coordination Compounds*. New York: 2nd Edition, Wiley Interscience Publication, pp. 252-254

Oktar, F. N., Agathopoulos, S., Ozyegin, L. S., Gunduz, O., Demirkol, M., Bozkurt, Y. and Salman, S. (2007). "Mechanical Properties of Bovine Hydroxyapatite (BHA) Composite Doped with SiO_2, MgO, Al_2O_3 and ZrO_2". *J. Mater Sci: Mater Med.*, vol. 18, pp. 2127-2143

Oliveira, M. and Mansur, H. S. (2007). "Synthetic Tooth Enamel: SEM Characterization of a Fluoride Hydroxyapatite Coating for Dentistry Applications". *Mater Res.,* vol. 10, pp. 115-118

Sadat-Shojai, M., Khorasani, M. T., Dinpanah-Khoshdargi, E. and Jamshidi, A. (2013). "Synthesis Methods for Nanosized Hydroxyapatite with Diverse Structures". *Acta Biomater*., vol. 9, pp.7591-7621

Sobczak, A., Kowalski, Z. and Wzorek, Z. (2009). "Preparation of Hydroxyapatite from Animal Bones". *Acta of Bioengineering and Biomechanics,* vol. 11(4), pp. 23-28

Sudipo, B. M., Apurba, P. and Sudit, M. (2012). "Studies on Processing and Characterizations of Hydroxyapatite Biomaterials from Different Bio Wastes". *Journal of Minerals and Materials Characterization and Engineering,* vol. 11(1), pp. 55-56

Than Than Khaing. (2006). *Process Development of Biocompatible Calcium Phosphate Powders from Waste Material (Egg shell)*. PhD Dissertation, Department of Chemistry, University of Yangon

Thin Thin Nwe, Kyaw Naing, Khin Mar Tun and Nyunt Wynn. (2005). "Preparation and Characterization of Apatitic Biphasic Calcium Phosphate". *Jour. Myan. Acad. Arts & Sc*., vol. 3(1), pp. 1-7

Zaw Moe Oo. (2014). *Preparation and Characterization of Hydroxyapatite from Fish Scale*. MSc Thesis, Department of Chemistry, University of Yangon